

# Bridging Modality Gap for Visual Grounding with Effective Cross-modal Distillation

Jiayi Wang<sup>a</sup>, Wenhui Hu<sup>a</sup>, Xueyang Liu<sup>a</sup>, Beihu Wu<sup>a</sup>, Yuting Qiu<sup>a</sup>,  
YingYing Cai<sup>a</sup>

<sup>a</sup>*Peking University, No.5 Yiheyuan Road Haidian District, Beijing, China*

---

## Abstract

Visual grounding aims to align visual information of specific regions of images with corresponding natural language expressions. Current visual grounding methods leverage pre-trained visual and language backbones separately to obtain visual features and linguistic features. Although these two types of features are then fused via delicately designed networks, the heterogeneity of the features makes them inapplicable for multi-modal reasoning. This problem arises from the domain gap between the single-modal pre-training backbone used in current visual grounding methods, which can hardly be overcome by the traditional end-to-end training method. To alleviate this, our work proposes an Empowering pre-trained model for Visual Grounding (EpmVG) framework, which distills a multimodal pre-trained model to guide the visual grounding task. EpmVG is based on a novel cross-modal distillation mechanism, which can effectively introduce the consistency information of images and texts in the pre-trained model, to reduce the domain gap existing in the backbone networks, thereby improving the performance of the model in the visual grounding task. Extensive experiments are carried out on five conventionally used datasets, and results demonstrate that our method achieves better performance than state-of-the-art methods.

*Keywords:* Visual grounding, Pre-trained model, Distillation

---

## 1. Introduction

Visual grounding [28, 36, 39], a key research area at the intersection of computer vision [45] and natural language processing [9], aims to link natural language descriptions to visual content by pinpointing the specific area of an

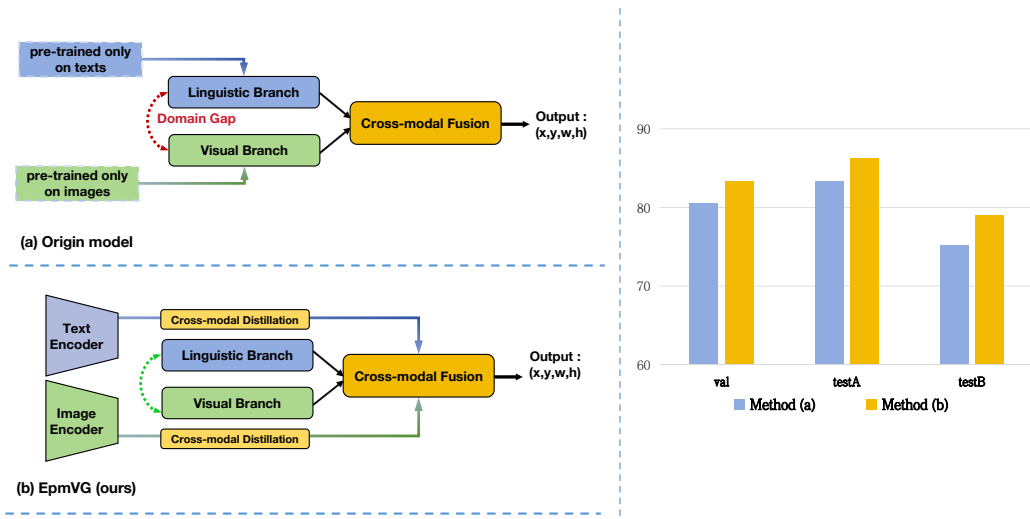


Figure 1: **Left:** (a) Basic visual grounding model and (b) our proposed EpmVG framework. **Right:** The comparison of two methods on the RefCOCO [62] dataset.

image described by the language. Unlike traditional object detection [42, 43] methods that can only identify limited categories in visual training data, visual grounding can detect novel categories and attributes expressed in free-form texts. This has garnered significant attention in recent years and has widespread applications like object search [24, 30], video analysis [29, 64, 65], automation [17], robot navigation [20], and augmented reality [10].

The early methods of visual grounding primarily focused on extending the application of one-stage and two-stage object detection architectures. One-stage methods [11, 25, 53, 59] utilize a pre-trained fully convolutional network (e.g., Darknet53 [42], ResNet [21]) to directly generate pixel-level feature maps and return the most likely candidate for the query text using manually defined dense anchors. These methods are simple and efficient for learning or inference, but they struggle with complex queries that involve multiple objects and relationships. Two-stage methods [36, 38, 49, 62] first generate a set of sparse region proposals and then exploit region-expression matching to find the best one. In these two-stage methods, modular attention networks [61], various graphs [54, 55], and multimodal trees [34] are designed to better model multimodal relationships. However, the complex fusion modules cannot be jointly learned with the detectors, which may limit

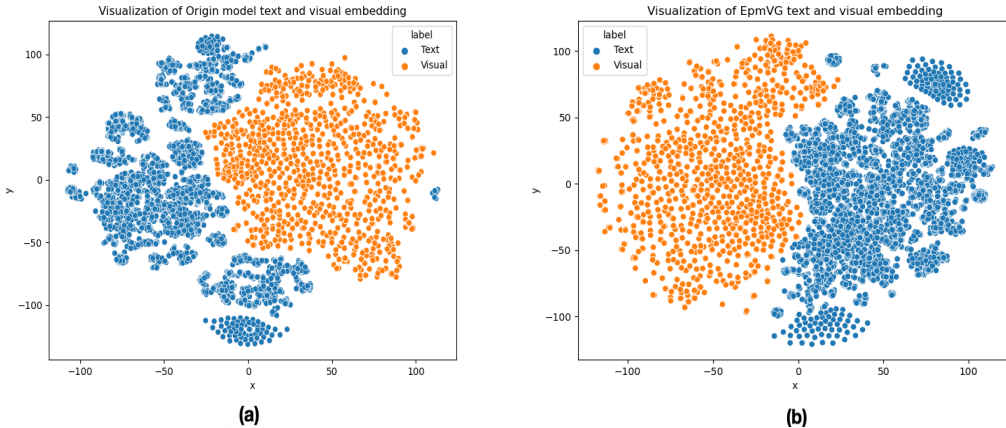


Figure 2: The comparison of the feature distribution representation of the two modalities using two methods on the RefCOCO [62] dataset. Where (a) Basic visual grounding model and (b) our proposed EpmVG framework.

their ability in multimodal reasoning. Recently, the visual grounding methods [2, 11, 53, 59] based on the Transformer [47] structure have been introduced into the field of visual localization due to their strong generalization ability and faster speed. It can perform more concise multi-modal reasoning based on pixel-level feature maps without the need for region proposals or dense anchor points. Most of the current state-of-the-art methods are based on the Transformer architecture. In this paper, we focus on designing a better Transformer-based visual grounding method.

Despite the success achieved by the existing Transformer-based visual grounding methods [11, 53, 59], we argue that they suffer from the **modality domain gap**. Specifically, during the pre-training stage, both the text and image encoder are pre-trained on their respective single-modal datasets. However, as shown in Figure 1 left(a), visual grounding is naturally a cross-modal task, and this domain gap may lead to inferior results.

In this paper, we propose an **E**mpowering **p**re-trained **m**odel for **V**isual **G**rounding (EpmVG) to address the domain gap issue. The proposed EpmVG can transfer the cross-modal correlation information contained in CLIP [41] by a novel **C**ross-modal **D**istillation loss (CD). We separately use the frozen CLIP [41] model’s visual encoder and text encoder to generate soft labels, which are used to constrain the corresponding visual branch

and linguistic branch. As depicted in Figure 1 left(b), EpmVG is capable of extracting correlation information from multi-modal inputs through pre-trained models. The experimental results shown in Figure 1 right(b) are better than the previous methods. The two modal feature distribution in Figure 2 indicate that it can guide the visual grounding model to reduce the modality domain gap between images and texts, facilitates cross-modal alignment between queries and related areas, and thereby enables accurate predictions. We evaluate our framework on five widely used visual grounding datasets, including ReferItGame [28], Flickr30K Entities [39], RefCOCO [62], RefCOCO+ [62], RefCOCOG [36], and our method effectively improves the performance of the original visual grounding method. Note that the proposed EpmVG can be easily applied to other visual grounding models. We use QR-Net [59] as our visual grounding model of EpmVG, which also significantly achieves absolute improvements over the original method and outperforms other existing methods.

The main contributions of this article are threefold:

- We analyze a problem existing in the current visual grounding tasks. Due to the domain gap issue in the pre-training stage, the visual and language backbones lack cross-modal correlation information between images and texts.
- We propose a framework EpmVG to transfer the correlation information of images and text to the visual grounding model through image-text joint distillation to improve the performance of the model.
- Extensive experiments are conducted to verify the advantages of our approach, and significantly improved results are shown on several popular benchmarks.

## 2. Related Work

### 2.1. Visual Grounding

The current visual grounding methods can be roughly classified into two categories, namely two-stage methods [6, 7, 22, 50, 59, 61] and one-stage methods [3, 5, 11, 27, 56–58].

**Two-stage methods.** The first stage involves generations of proposals, which are candidate regions containing objects in images that can be selected in the next stage. In the second stage, the matching similarities between the

region proposal and text expressions will be measured and leveraged to perform a ranking task. The best-matched proposal thus can be found. Some works focus on the second stage to improve the model performance. MAttNet [61] and RvG-Tree [22] draw on the logical or structural decomposition of language expression to better reason the fine-grained linguistic information, to more accurately construct alignment with visual features. Another work [50] also exploits a graph-based attention mechanism to capture both the object’s attributes and its relationships to other objects in the expressions. However, the features proposed by the first stage may not contain the information the second stage needs, and such a gap makes the optimization in the second stage futile. To solve this, Ref-NMS [7] in the first stage generates proposals aware of specific expressions by selecting nouns as critical objects. QRNet [59] further alleviates this problem by replacing the query-agnostic visual module with a query-aware module, thus providing more representative features for multimodal reasoning.

**One-stage methods.** The one-stage method aims to overcome the weakness of the two-stage method by eliminating the possibility of the malfunctions in first stage. By fusing expression features with visual features, it can directly predict target objects position with bounding boxes. Yang et al. [57] embed text query to a 768D vector with a BERT [12] model and extract visual features with Darknet-53 [42], and then they perform feature fusion by broadcasting and concatenating text features with visual and spatial features. Yang et al. [56] proposes to reduce the ambiguity of reference by identifying sub-query information, instead of using single vector representation to embed the entire sentences. To improve cross-modal understanding of modal, Ye et al. [58] use three filters of three dimensions to filter visual features in corresponding to different facets of a text query, which are obtained by taking structural and contextual information into account.

**Transformer-based Method.** Dosovitskiy et al.’s pioneer ViT [13] shows that pure transformer frameworks can effectively perform image classification tasks. Recent works like TTSR by Yang et al. [52] and Deformable DETR by Zhu et al. [67] use transformers for specific vision tasks like image super-resolution and small object detection. To improve the performance of ViT, Liu et al. [35] proposed a new hierarchical ViT called Swin transformer. These transformer-based visual backbones provide support for visual grounding models. TransVG [11] and MDETR [27] both draw on the transformer to solve the problem of overfitting in certain scenarios and a long tail of open and free textual expressions respectively. QRNet [59] employs

a Swin encoder to extract visual features and proposes a fine-grained query modulation visual grounding framework.

## 2.2. Knowledge Distillation

Knowledge Distillation [16] aims at scaling down large models with huge amounts of parameters, to make it possible to achieve similar task performance with fewer resources. It usually involves training a student model by utilizing the knowledge of a teacher model. Some work [1, 4] studies how to improve model performance by using different ways of distillation. To facilitate the application of ViT, Touvron et al. [46] take the distillation method, which involves training a student transformer by a powerful teacher image classifier, thus scaling the training work down with less data. In order to address the lack of large-scale training data for open-vocabulary text-visual tasks, ViLD [19] performs distillation by using pre-trained open-vocabulary image classification models, like CLIP [41] and ALIGN [26], as a teacher and modifying a vanilla detector as a student. Its detection categories are up to more than 1000 compared with tens of that of previous methods.

## 3. Method

In this work, we propose to transfer the visual and linguistic knowledge contained in the pre-trained model into a visual grounding model, namely **E**mpowering **P**re-trained **M**odel for **V**isual **G**rounding (EpmVG). The EpmVG structure is shown in Figure 3. There are two main components in EpmVG: (1) a visual grounding model, and (2) a distillation module. In the following subsections, we first formulate the visual grounding task and then introduce the architecture of EpmVG.

### 3.1. Visual Grounding Module

The main purpose of the visual grounding task is to map a query to a specific region of the image. This query corresponds to an object in the image, which can be a sentence or a phrase. The task can be defined as follows: given an image  $I$  and a query  $q$ , the model needs to predict a bounding box  $\mathbf{b} = \{x, y, w, h\}$  that accurately surrounds the target object described by the query.

As shown in Figure 3, our visual grounding model is designed based on a typical end-to-end visual grounding architecture TransVG [11]. There are

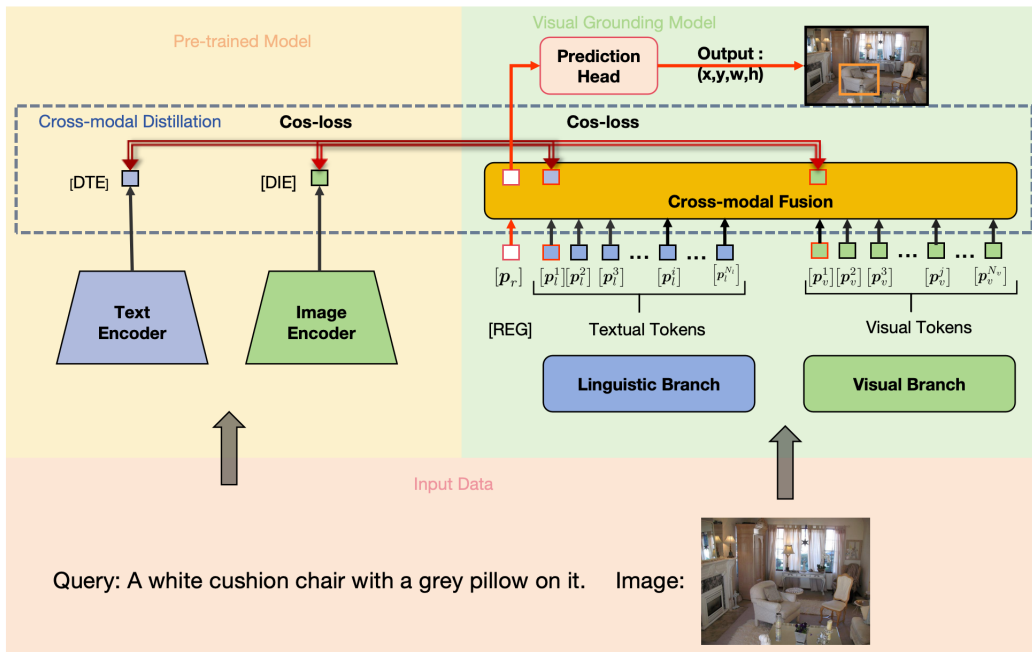


Figure 3: An overview of EpmVG framework. It consists of two main components: (1) a visual grounding model; and (2) a distillation module.

four main components in our visual grounding model: (1) a visual branch, (2) a linguistic branch, (3) a cross-modal fusion, and (4) a prediction module.

**Visual Branch.** The vision branch starts with a convolutional backbone network, followed by a vision transformer. We utilize the commonly used ResNet [21] as the backbone network. The vision transformer is a stack of transformer encoder layers. Each transformer encoder layer consists of a multi-head self-attention layer and an FFN.

First, the visual branch input is an image  $\mathbf{z}_0 \in \mathbb{R}^{3 \times H_0 \times W_0}$ , and then the backbone network is used to generate a two-dimensional feature map  $\mathbf{z} \in \mathbb{R}^{C \times H \times W}$ .

Then, this branch uses the  $1 \times 1$  convolutional layer to reduce the dimension of channels of  $\mathbf{z}$ , and obtain  $\mathbf{z}' \in \mathbb{R}^{C_v \times H \times W}$ . In order to conform to the input format of the transformer encoding layer,  $\mathbf{z}'$  is flattened to  $\mathbf{z}_v \in \mathbb{R}^{C_v \times N_v}$ , where  $N_v = H \times W$  is the number of input tokens. Finally, the visual transformer extracts the visual context features and outputs the visual embedding  $\mathbf{f}_v$ , which has the same shape as  $\mathbf{z}_v$ .

**Linguistic Branch.** We utilize the linguistic branch, typically implemented as a pre-trained BERT [12] model, to encode the query sentence. The language embedding is denoted as  $\mathbf{f}_l \in \mathbb{R}^{C_l \times N_l}$ , where  $N_l$  is the number of language tokens.

**Cross-modal Fusion.** The core structure of this module is a visual-linguistic transformer. To make the feature embeddings of different modalities have the same dimensions, we apply a linear projection layer to map them into embeddings with the same channel dimensions  $\mathbb{R}^D$ . The projected visual and linguistic features are denoted by  $\mathbf{p}_v \in \mathbb{R}^{D \times N_v}$  and  $\mathbf{p}_l \in \mathbb{R}^{D \times N_l}$ . Then,  $\mathbf{p}_v$  and  $\mathbf{p}_l$  are connected by inserting a learnable embedding (namely a [REG] token) at the beginning of the connection sequence, and formulate the joint input tokens of the visual-linguistic transformer as:

$$\mathbf{X} = [\mathbf{p}_r, \mathbf{p}_v, \mathbf{p}_l], \quad (1)$$

$$\mathbf{p}_v = [\mathbf{p}_v^1, \mathbf{p}_v^2, \dots, \mathbf{p}_v^{N_v}], \quad (2)$$

$$\mathbf{p}_l = [\mathbf{p}_l^1, \mathbf{p}_l^2, \dots, \mathbf{p}_l^{N_l}], \quad (3)$$

where  $\mathbf{p}_r$  represents the learnable embedding of [REG] token,  $\mathbf{p}_v$  represents the visual tokens and  $\mathbf{p}_l$  represents the linguistic tokens.  $\mathbf{p}_l^1$  is the [CLS] token’s representation which is regarded as the contextual textual feature. And  $\mathbf{p}_v^1$  is denoted by [VLS] which is regarded as the global visual feature.

After obtaining the input  $\mathbf{X} \in \mathbb{R}^{D \times (N_v + N_l + 1)}$  in the joint embedding space as mentioned above, we apply a multi-layer visual-linguistic transformer to perform intra- and inter-modal reasoning on the joint sequence through an attention mechanism. Finally, we obtain the output of this module  $\mathbf{X}' = [\mathbf{p}'_r, \mathbf{p}'_v^1, \mathbf{p}'_v^2, \dots, \mathbf{p}'_v^{N_v}, \mathbf{p}'_l^1, \mathbf{p}'_l^2, \dots, \mathbf{p}'_l^{N_l}] \in \mathbb{R}^{D \times (N_v + N_l + 1)}$ .

**Prediction Module.** Finally, a prediction module is used to handle the output representation of the [REG] token from the Cross-modal Fusion module. The primary task of this prediction module is to predict the coordinates of the bounding box  $\mathbf{b}$  based on this output representation. In short, the computing process is formulated as follows:

$$\begin{aligned} \mathbf{p}'_r &= \text{ReLU}(\text{MLP}(\text{ReLU}(\text{MLP}(\mathbf{p}'_r))))), \\ \mathbf{p}'_r &= \text{MLP}(\mathbf{p}'_r), \\ \mathbf{b} &= \text{Sigmoid}(\mathbf{p}'_r). \end{aligned} \quad (4)$$



### 3.2. Cross-modal Distillation Module

In this section, we introduce the proposed framework of EpmVG. We utilize CLIP [41] as our pre-trained model. Because the CLIP [41] model uses a large number of image and text pairs for training, the model can understand the semantic relationship between images and text. For example, given an image and a text describing the image, a CLIP [41] model can understand the relationship between the two and apply this understanding to new images and text. The visual grounding task relies heavily on the model’s understanding of the semantic relationship between images and text. In the EpmVG, we utilize Cross-modal Distillation loss to effectively transfer the pre-trained model’s understanding of the semantic relationship between images and text to the visual grounding model, the details of which are shown as follows.

For a given image  $\mathbf{z}_0 \in \mathbb{R}^{3 \times H_0 \times W_0}$ , we utilize CLIP [41]’s image encoder to extract one-dimensional features  $\hat{\mathbf{p}}_{cv} \in \mathbb{R}^d$  that incorporate visual semantic information and corresponding text relationship information, where  $\hat{\mathbf{p}}_{cv}$  is named [DIE]. To the same, for a given query sentence, we utilize CLIP [41]’s text encoder to extract one-dimensional features  $\hat{\mathbf{p}}_{cl} \in \mathbb{R}^d$  that incorporate textual semantic information and corresponding visual relationship information, where  $\hat{\mathbf{p}}_{cl}$  is named [DTE]. Then we utilize  $\hat{\mathbf{p}}_{cv}$  and  $\hat{\mathbf{p}}_{cl}$  to guide at the beginning positions of the tokenized image expression  $\mathbf{p}'_v$  and at the beginning positions of the tokenized language expression  $\mathbf{p}'_l$  to better acquire the knowledge of the semantic relationship between images and text in the pre-trained model. The distillation process is formulated as:

$$\hat{\mathbf{P}}_{cv} = \text{AvgPool}(\hat{\mathbf{p}}_{cv}, \mathbf{p}'_v), \quad (5)$$

$$\hat{\mathbf{P}}_{cl} = \text{AvgPool}(\hat{\mathbf{p}}_{cl}, \mathbf{p}'_l), \quad (6)$$

We utilize Adaptive Average Pooling [51] to transform  $\hat{\mathbf{p}}_{cv}$  into the same dimension as  $\mathbf{p}'_v$ . The same operation is also applied to  $\hat{\mathbf{p}}_{cl}$ . Where  $\hat{\mathbf{P}}_{cv} \in \mathbb{R}^D$  and  $\hat{\mathbf{P}}_{cl} \in \mathbb{R}^D$  are the feature(s) after transformation.

$$\mathcal{L}_{\text{distillation}} = \alpha \cdot \mathcal{L}_{\text{cos}}(\mathbf{p}'_v, \hat{\mathbf{P}}_{cv}) + \beta \cdot \mathcal{L}_{\text{cos}}(\mathbf{p}'_l, \hat{\mathbf{P}}_{cl}), \quad (7)$$

where  $\mathcal{L}_{\text{cos}}(\cdot)$  is the cosine loss [48],  $\alpha$  and  $\beta$  are the distillation weights for balancing the two modalities.

Finally, we get both the prediction module’s prediction  $\mathbf{b} = (x, y, w, h)$ , and the normalized ground-truth box as  $\hat{\mathbf{b}} = (\hat{x}, \hat{y}, \hat{w}, \hat{h})$ . And the training objective of our EpmVG is:

$$\mathcal{L} = \mathcal{L}_{\text{smooth-11}}(\mathbf{b}, \hat{\mathbf{b}}) + \lambda \cdot \mathcal{L}_{\text{giou}}(\mathbf{b}, \hat{\mathbf{b}}) + \mathcal{L}_{\text{distillation}}, \quad (8)$$

where  $\mathcal{L}_{\text{smooth-l1}}(\cdot)$  and  $\mathcal{L}_{\text{giou}}(\cdot)$  are the smooth L1 loss [15] and GIoU loss [44], respectively.  $\lambda$  is the weight coefficient of GIoU loss to balance these losses.

## 4. Experiments

### 4.1. Datasets and Evaluation

**ReferItGame.** The ReferItGame [28] dataset contains 120,072 expressions and 19,997 natural-scene images, and all the images have 96,654 distinct objects in total that can be referred to by the mentioned expressions. This dataset is built upon the ImageCLEF IAPR [18] image retrieval dataset and the SAIAPR TC-12 [14] expansion. Such basis empowers this dataset to cover a wide range of daily life objects such as people, animals, and cities, and to label objects in diverse dimensions like location, size, and category of those objects. Following the practice of previous works like [11, 59], we allocate the data to three parts: 54,127 referring expressions for training, 5,842 referring expressions for validation and 60,103 referring expressions for test.

**Flickr30K Entities.** Flickr30k Entities [39] is a dataset constructed on the basis of Flickr30k [60] for image description, with one or several captions identifying one or several entities or scenes in pictures. One of its most valuable features is that it gives the ground truth of the specific locations of the mentioned entities. In total, it contains 31,783 images of people, clothing, body parts, and animals etc., and 158,915 English captions (five per image). For each set of captions for one image, there are several mentions refer to one type entities corresponding to the mentions, thus creating 244,035 coreference chains. And 275,775 bounding boxes are identified on all the images to show where the mentioned entities are. This dataset is divided into three parts, a train set containing 29,783 images, a validation set containing 1000 images, and a test set containing 1000 images.

**RefCOCO/ RefCOCO+/ RefCOCOg.** The three datasets are all based on Microsoft COCO [32] and they contain images with 80 categories of common objects. RefCOCO [62] and RefCOCO+ [62] are built on ReferItGame. One player describes one object in an image and the other chooses one object according to the expression of the first player. If the choice and the target object matches, they earn points and exchange roles, otherwise they move on to the next image. One distinction between the two datasets is that RefCOCO+ [62] forbids players from using location words. RefCOCOg [36]

is constructed on Amazon Mechanical Turk. Its process is similar to Refer-ItGame, but without the interaction part. RefCOCO [62] has 19,994 images with 50,000 objects depicted by 142,209 refer expressions, RefCOCO+ [62] includes 19,992 images with 49,856 objects described by 141,564 expressions, and RefCOCOg [36] contains 26,711 images with 54,822 objects referred by 85,474 expressions. For the dataset partition for training, validation and testing, we follow the official and conventional practice as in [11].

**Evaluation Metric.** We adopt the same evaluation metrics as [11]. Specifically, if the Intersection over Union (IoU) of the predicted bounding box and the actual (ground-truth) bounding box exceeds 0.5, then this prediction is considered to be correct.

#### 4.2. Implementation Details

The dimensions of the input image are established at  $H_o = 640$  and  $W_o = 640$ . In the process of resizing the image, the original aspect ratio is maintained. The image’s longer side is adjusted to 640, and the shorter side is padded to 640 using the average value of the RGB channels. Meanwhile, for language queries, we set the maximum length to 40 for RefCOCOg, and to 20 for other datasets.

During training, we use the CLIP [41] model as the pre-trained model component of our EpmVG framework. We adhere to the procedures outlined in TransVG [11] for processing input images and sentences. Similarly, we adopt the training configuration utilized in TransVG, which employs an AdamW optimizer with a weight decay of  $10^{-4}$ , establishes a batch size of 64, and sets a dropout ratio of 0.1 for the FFN in the Transformer. The learning rate for pre-trained parameters in the visual and linguistic branch is set at  $10^{-5}$ , while it is set at  $10^{-4}$  for the remaining parameters. The parameters without pre-training are randomly initialized with Xavier. We train our model 180 epochs (with a corresponding learning rate drop at 120) for RefCOCO+, and 90 epochs (with a corresponding learning rate drop at 60) for other datasets. The weight coefficient  $\gamma$  is set to 1. The distillation weight coefficients  $\alpha$  and  $\beta$  are set to 1.5 and 2. We also adopt the data augmentation strategies commonly employed in [31, 56, 57].

#### 4.3. Ablation Study

In this section, we conducted a series of ablation experiments to validate the effectiveness of our proposed framework and each of its components. Initially, we selected different methods as our visual grounding module and

Table 1: Comparison with the method without distillation on the test set of ReferItGame [28] and Flickr30K [39] Entities in terms of top-1 accuracy (%).

VG method	Backbone	Distillation	ReferItGame test	Flickr30K test	RefCOCO		
					val	testA	testB
TransVG	ResNet-50	w/o	69.76	78.47	80.49	83.28	75.24
		w/	<b>70.65</b>	<b>79.29</b>	<b>83.39</b>	<b>86.20</b>	<b>78.98</b>
TransVG	ResNet-101	w/o	70.73	79.10	80.83	83.38	76.94
		w/	<b>71.16</b>	<b>79.58</b>	<b>82.49</b>	<b>85.23</b>	<b>79.51</b>
QRNet	Swin-S	w/o	74.61	81.95	84.01	85.85	82.34
		w/	<b>75.84</b>	<b>83.14</b>	<b>87.04</b>	<b>89.21</b>	<b>82.90</b>

Table 2: Comparisons with state-of-the-art methods on RefCOCO [62], RefCOCO+ [62] and RefCOCOg [36] in terms of top-1 accuracy (%).

VG method	Backbone	Distillation	RefCOCO+			RefCOCOg		
			val	testA	testB	val-g	val-u	test-u
TransVG	ResNet-50	w/o	66.39	70.55	57.66	66.35	67.93	67.44
		w/	<b>69.67</b>	<b>74.70</b>	<b>59.87</b>	<b>71.61</b>	<b>71.92</b>	<b>71.40</b>
TransVG	ResNet-101	w/o	68.00	72.46	59.24	68.03	68.71	67.98
		w/	<b>69.34</b>	<b>73.57</b>	<b>60.85</b>	<b>69.54</b>	<b>71.02</b>	<b>70.74</b>
QRNet	Swin-S	w/o	72.94	76.17	63.81	71.89	73.03	72.52
		w/	<b>76.45</b>	<b>81.16</b>	<b>68.12</b>	<b>76.15</b>	<b>79.32</b>	<b>76.61</b>

compared the performance of the model before and after distillation on five widely used public datasets to verify the effectiveness of our proposed framework.

**Effectiveness of the Overall Framework.** The overall effectiveness of the framework was demonstrated by constructing the visual grounding part of EpmVG based on TransVG [11] and QRNet [59] methods and comparing the results before and after distillation on five public datasets. As shown in Tables 1 and 2, our method significantly outperformed the original methods on all five datasets after adding cross-modal distillation module, effectively validating the efficacy of our framework.

Next, we validated the effectiveness of each component of the framework on the RefCOCO [62] dataset, where the VG model was based on TransVG [11], and the backbone network was ResNet-50.

**Distillation Loss.** As shown in Table 3, we studied the effectiveness of the distillation loss function and multimodal distillation in cross-modal distillation module. When cos loss was replaced with L1 loss, the performance decreased by 0.96%, 1.39%, and 1.55% on val, testA, and testB, respectively,

Table 3: Ablation studies of distillation loss function and distillation modes in EpmVG.

Mode	Distillation	Image	Text	RefCOCO		
	Loss	Distillation	Distillation	val	testA	testB
#1	Cos.	✓	✓	<b>83.39</b>	<b>86.20</b>	<b>78.98</b>
#2	L1	✓	✓	82.43	84.81	77.43
#3	Cos.	✓	×	70.28	60.92	54.33
#4	Cos.	×	✓	72.75	62.37	55.23

indicating that cos loss is more effective than L1 loss. When text modality distillation was removed, the performance decreased by 13.11%, 25.28%, and 24.65%, respectively. When image modality distillation was removed, the performance decreased by 10.64%, 23.83%, and 23.75%, respectively. We found that the distillation of both modalities is crucial, and only by distilling both text and images can we more effectively learn the semantic consistency information in the pre-trained model.

**Distillation Location.** We also validated the impact of different distillation locations on model performance. As shown in Table 4, Loc.1 represents distillation at the last layer of Cross-modal Fusion; Loc.2 represents distillation at the two Branches’ Linear layers; Loc.3 represents distillation at the last layer of the transformers in the two Branches; Loc.4 represents distillation at the CNN of the Visual Branch and the embedding layer of the Linguistic Branch. Through the experimental results, we found that the closer the distillation position is to the input end, the more significant the performance decline, which also proves the effectiveness of our choice to distill in the cross-modal fusion module. For a better understanding, a location diagram is provided in the appendix.

**Pretrained Model Parameters.** We experimentally validated the impact of whether the parameters of the pre-training model CLIP [41] are frozen during the distillation process on performance. As shown in Table 5, when the parameters were not frozen, the performance decreased by 0.36%, 0.93%, and 0.94%, respectively. This suggests that if the CLIP [41] model is altered during the distillation process, it may cause the knowledge learned by the VG model to change, thereby affecting its performance.

#### 4.4. Comparisons with State-of-the-art Methods

We present the comparison results on ReferItGame [28] and Flickr30k [39] Entities in Table 6. ReferItGame is a cooperative game that gathers queries

Table 4: Ablation studies of distillation location in EpmVG. Loc.1 represents distillation at the last layer of Cross-modal Fusion; Loc.2 represents distillation at the two Branches’ Linear layers; Loc.3 represents distillation at the last layer of the transformers in the two Branches; Loc.4 represents distillation at the CNN of the Visual Branch and the embedding layer of the Linguistic Branch. Please refer to Figure A.5 in the appendix for detailed information.

Mode	Distillation Location	RefCOCO		
		val	testA	testB
#1	Loc.1	<b>83.39</b>	<b>86.20</b>	<b>78.98</b>
#2	Loc.2	81.61	84.38	76.43
#3	Loc.3	80.89	83.30	75.06
#4	Loc.4	80.13	83.07	76.08

Table 5: Ablation studies of whether the pre-trained model is frozen in EpmVG.

Mode	Pretrained Model Parameters	RefCOCO		
		val	testA	testB
#1	frozen	<b>83.39</b>	<b>86.20</b>	<b>78.98</b>
#2	unfrozen	83.03	85.27	78.04

by having one player create a referential phrase for a designated object, while another player is tasked with selecting the correct object. As for Flickr30k Entities, the queries are derived from the phrases found in the title. We observe that the proposed EpmVG surpasses previous work. The cross-modal distillation we designed effectively introduces the semantic consistency information of images and text in CLIP [41] into the VG model. This solves the problem of the domain gap between the single-modal pre-training of the backbone network and the downstream multi-modal tasks in the VG model that we mentioned earlier, successfully improving accuracy.

We also show the accuracy comparison with state-of-the-art methods on ReferCOCO [62], ReferCOCO+ [62], and ReferCOCog [36] in Table 7. In the ReferCOCO and ReferCOCO+ datasets, the referred objects in “testA” are people, and in “testB” they may be common objects. The expressions in ReferCOCog are much longer than those in other datasets. According to the experimental results, our EpmVG performs excellently among all two-stage and one-stage state-of-the-art methods. On the ReferCOCO and ReferCOCO+ datasets, our method gains 3.36%~4.99% absolute improvement in “testA” and 0.56%~4.31% in “testB”. In the RefCOCog test split with longer expressions, our method is also effective, gaining 4.09% improvement.

Table 6: The performance comparisons (Acc@0.5) on ReferItGame [28] and Flickr30K Entities [39].

Models	Backbone	ReferItGame test	Flickr30K test
<b><i>Two-stage:</i></b>			
VC [66]	VGG16	31.13	-
MAttNet [61]	ResNet-101	29.04	-
Similarity Net [49]	ResNet-101	34.54	60.89
DDPN [63]	ResNet-101	63.00	73.30
DIGN [37]	VGG-16	65.15	78.73
<b><i>One-stage:</i></b>			
FAOA [57]	DarkNet-53	60.67	68.71
RCCF [31]	DLA-34	63.79	-
ReSC-Large [56]	DarkNet-53	64.60	69.28
TransVG [11]	ResNet-101	70.73	79.10
TransVG (Swin)	Swin-S	70.86	78.18
QRNet [59]	Swin-S	74.61	81.95
EpmVG(ours)	Swin-S	<b>75.84</b>	<b>83.14</b>

This indicates that our proposed cross-modal distillation is very stable and effective, and also demonstrates the importance of the semantic consistency information of images and text in visual grounding tasks.

#### 4.5. Qualitative Results

We present a qualitative comparison between our EpmVG and three popular methods in Figure 4. We observe that our method can successfully model more complex queries, such as “woman in tan jacket talking to lady in purple jacket” in Figure 4. We can see that previous methods are not able to understand the correspondence between complex queries and objects in the image well, leading to incorrect predictions, such as the results of TransVG [11] and QRNet [59] for the queries of “blurry man with cap holding railing” and “green colored goggles looking at camera”. In contrast, our EpmVG generates query-consistent features by our designed cross-modal distillation and makes more accurate predictions. This cross-modal distillation can introduce the image-text consistency information contained in the CLIP [41] model, helping the model to better understand the relationship between the query and the image, thereby generating more accurate features and reducing the sensitivity to query-unrelated areas. More results can be found in the appendix.

Table 7: The performance comparisons (Acc@0.5) on ReferCOCO [62], ReferCOCO+ [62], and ReferCOCOg [36]. The results of previous best two-stage and one-stage methods are highlighted with underlines. We highlight our results in bold. The results demonstrate that our method outperforms all state-of-the-art one-stage and two-stage methods.

Models	Backbone	RefCOCO			RefCOCO+			RefCOCOg		
		val	testA	testB	val	testA	testB	val-g	val-u	test-u
<b><i>Two-stage:</i></b>										
CMN [23]	VGG16	-	71.03	65.77	-	54.32	47.76	57.47	-	-
VC [66]	VGG16	-	73.33	67.44	-	58.40	53.18	62.30	-	-
MAttNet [61]	ResNet-101	<u>76.65</u>	81.14	69.99	<u>65.33</u>	71.62	56.02	-	66.58	67.27
LGRANs [50]	VGG16	-	76.60	66.40	-	64.00	53.40	61.78	-	-
DGA [54]	VGG16	-	78.42	65.53	-	69.07	51.99	-	-	63.28
RvG-Tree [22]	ResNet-101	75.06	78.61	69.85	63.51	67.45	56.66	-	66.95	66.51
NMTree [33]	ResNet-101	76.41	81.21	70.09	66.46	72.02	57.52	64.62	65.87	66.44
<b><i>One-stage:</i></b>										
SSG [8]	DarkNet-53	-	76.51	67.50	-	62.14	49.27	47.47	58.80	-
FAOA [57]	DarkNet-53	72.54	74.35	68.50	56.81	60.23	49.60	56.12	61.33	60.36
RCCF [31]	DLA-34	-	81.06	71.85	-	70.35	56.32	-	-	65.73
ReSC-Large [56]	DarkNet-53	77.63	80.45	72.30	63.59	68.36	56.81	63.12	67.30	67.20
SAFF [58]	DarkNet-53	79.26	81.09	76.55	64.43	68.46	58.43	-	68.94	68.91
HFRN [40]	ResNet-101	79.76	83.12	75.51	66.80	72.53	59.09	-	69.71	69.08
LBYL-Net [25]	DarkNet-53	79.67	82.91	74.15	68.64	73.38	59.49	62.70	-	-
TransVG[11]	ResNet-101	81.02	82.72	78.35	64.82	70.70	56.94	67.02	68.67	67.73
TransVG (Swin)	Swin-S	82.33	84.01	79.83	64.94	70.19	56.47	67.81	69.34	68.99
QRNet [59]	Swin-S	<u>84.01</u>	<u>85.85</u>	<u>82.34</u>	<u>72.94</u>	<u>76.17</u>	<u>63.81</u>	<u>71.89</u>	<u>73.03</u>	<u>72.52</u>
EpmVG (ours)	Swin-S	<b>87.04</b>	<b>89.21</b>	<b>82.90</b>	<b>76.45</b>	<b>81.16</b>	<b>68.12</b>	<b>76.15</b>	<b>79.32</b>	<b>76.61</b>

## 5. Conclusion

In this paper, we argue that the visual and linguistic backbone used in current visual grounding methods has a modality domain gap since they are separately pre-trained with one single modality. To overcome this weakness, we propose EpmVG, which aims to empower the pre-trained model for visual grounding. Specifically, we propose a novel cross-modal distillation mechanism, which effectively distills the cross-modal information within the CLIP model, thus reducing the existing domain gap and improving the grounding performance. Extensive experiments indicate that the proposed framework significantly outperforms the state-of-the-art methods.





Figure 4: Qualitative comparison with TransVG [11] and QRNet [59]. Green boxes are the ground-truth, yellow boxes are the predictions.

## Acknowledgements

## References

- [1] Abnar, S., Dehghani, M., Zuidema, W., 2021. Transferring inductive biases through knowledge distillation. arXiv: Learning,arXiv: Learning .
- [2] Cao, M., Chen, L., Shou, M.Z., Zhang, C., Zou, Y., 2021. On pursuit of designing multi-modal transformer for video grounding, in: Proceedings of the 2021 Conference on Empirical Methods in Natural Language Processing, pp. 9810–9823.
- [3] Cao, M., Jiang, J., Chen, L., Zou, Y., 2022a. Correspondence matters

for video referring expression comprehension, in: Proceedings of the 30th ACM International Conference on Multimedia, pp. 4967–4976.

- [4] Cao, M., Wei, F., Xu, C., Geng, X., Chen, L., Zhang, C., Zou, Y., Shen, T., Jiang, D., 2023. Iterative proposal refinement for weakly-supervised video grounding, in: Proceedings of the IEEE/CVF Conference on Computer Vision and Pattern Recognition, pp. 6524–6534.
- [5] Cao, M., Yang, T., Weng, J., Zhang, C., Wang, J., Zou, Y., 2022b. Locvtp: Video-text pre-training for temporal localization, in: European Conference on Computer Vision, Springer. pp. 38–56.
- [6] Cao, M., Zhang, C., Chen, L., Shou, M.Z., Zou, Y., 2022c. Deep motion prior for weakly-supervised temporal action localization. *IEEE Transactions on Image Processing* 31, 5203–5213.
- [7] Chen, L., Ma, W., Xiao, J., Zhang, H., Chang, S.F., 2021. Ref-nms: Breaking proposal bottlenecks in two-stage referring expression grounding, in: Proceedings of the AAAI Conference on Artificial Intelligence, pp. 1036–1044.
- [8] Chen, X., Ma, L., Chen, J., Jie, Z., Liu, W., Luo, J., 2018. Real-time referring expression comprehension by single-stage grounding network. arXiv preprint arXiv:1812.03426 .
- [9] Chowdhary, K., Chowdhary, K., 2020. Natural language processing. *Fundamentals of artificial intelligence* , 603–649.
- [10] Craig, A.B., 2013. Understanding augmented reality: Concepts and applications .
- [11] Deng, J., Yang, Z., Chen, T., Zhou, W., Li, H., 2021. Transvg: End-to-end visual grounding with transformers. arXiv preprint arXiv:2104.08541 .
- [12] Devlin, J., Chang, M.W., Lee, K., Toutanova, K., 2018. Bert: Pre-training of deep bidirectional transformers for language understanding. arXiv preprint arXiv:1810.04805 .
- [13] Dosovitskiy, A., Beyer, L., Kolesnikov, A., Weissenborn, D., Zhai, X., Unterthiner, T., Dehghani, M., Minderer, M., Heigold, G., Gelly, S.,

- et al., 2020. An image is worth 16x16 words: Transformers for image recognition at scale. arXiv preprint arXiv:2010.11929 .
- [14] Escalante, H.J., Hernández, C.A., Gonzalez, J.A., López-López, A., Montes, M., Morales, E.F., Sucar, L.E., Villasenor, L., Grubinger, M., 2010. The segmented and annotated iapr tc-12 benchmark. *Computer vision and image understanding* 114, 419–428.
  - [15] Girshick, R., 2015. Fast r-cnn, in: *Proceedings of the IEEE international conference on computer vision*, pp. 1440–1448.
  - [16] Gou, J., Yu, B., Maybank, S.J., Tao, D., 2021. Knowledge distillation: A survey. *International Journal of Computer Vision* , 1789–1819.
  - [17] Groover, M.P., 2001. *Automation. Production Systems and Computer Integrated Manufacturing* 2.
  - [18] Grubinger, M., Clough, P., Müller, H., Deselaers, T., 2006. The iapr tc-12 benchmark: A new evaluation resource for visual information systems, in: *International workshop ontoImage*.
  - [19] Gu, X., Lin, T.Y., Kuo, W., Cui, Y., 2021. Open-vocabulary object detection via vision and language knowledge distillation. *Learning, Learning* .
  - [20] Gul, F., Rahiman, W., Nazli Alhady, S.S., 2019. A comprehensive study for robot navigation techniques. *Cogent Engineering* 6, 1632046.
  - [21] He, K., Zhang, X., Ren, S., Sun, J., 2016. Deep residual learning for image recognition, in: *Proceedings of the IEEE conference on computer vision and pattern recognition*, pp. 770–778.
  - [22] Hong, R., Liu, D., Mo, X., He, X., Zhang, H., 2019. Learning to compose and reason with language tree structures for visual grounding. *IEEE transactions on pattern analysis and machine intelligence* .
  - [23] Hu, R., Rohrbach, M., Andreas, J., Darrell, T., Saenko, K., 2017. Modeling relationships in referential expressions with compositional modular networks, in: *Proceedings of the IEEE Conference on Computer Vision and Pattern Recognition*, pp. 1115–1124.

- [24] Hu, R., Xu, H., Rohrbach, M., Feng, J., Saenko, K., Darrell, T., 2016. Natural language object retrieval, in: Proceedings of the IEEE Conference on Computer Vision and Pattern Recognition, pp. 4555–4564.
- [25] Huang, B., Lian, D., Luo, W., Gao, S., 2021. Look before you leap: Learning landmark features for one-stage visual grounding, in: Proceedings of the IEEE/CVF Conference on Computer Vision and Pattern Recognition, pp. 16888–16897.
- [26] Jia, C., Yang, Y., Xia, Y., Chen, Y.T., Parekh, Z., Pham, H., Le, Q., Sung, Y.H., Li, Z., Duerig, T., 2021. Scaling up visual and vision-language representation learning with noisy text supervision. Cornell University - arXiv, Cornell University - arXiv .
- [27] Kamath, A., Singh, M., LeCun, Y., Synnaeve, G., Misra, I., Carion, N., 2021. Mdetr-modulated detection for end-to-end multi-modal understanding, in: Proceedings of the IEEE/CVF International Conference on Computer Vision, pp. 1780–1790.
- [28] Kazemzadeh, S., Ordonez, V., Matten, M., Berg, T., 2014. Referitgame: Referring to objects in photographs of natural scenes, in: Proceedings of the 2014 conference on empirical methods in natural language processing (EMNLP), pp. 787–798.
- [29] Li, H., Cao, M., Cheng, X., Li, Y., Zhu, Z., Zou, Y., 2023. G2l: Semantically aligned and uniform video grounding via geodesic and game theory, in: Proceedings of the IEEE/CVF International Conference on Computer Vision, pp. 12032–12042.
- [30] Li, J., Wei, Y., Liang, X., Zhao, F., Li, J., Xu, T., Feng, J., 2017. Deep attribute-preserving metric learning for natural language object retrieval, in: Proceedings of the 25th ACM international conference on Multimedia, pp. 181–189.
- [31] Liao, Y., Liu, S., Li, G., Wang, F., Chen, Y., Qian, C., Li, B., 2020. A real-time cross-modality correlation filtering method for referring expression comprehension, in: Proceedings of the IEEE/CVF Conference on Computer Vision and Pattern Recognition, pp. 10880–10889.
- [32] Lin, T.Y., Maire, M., Belongie, S., Hays, J., Perona, P., Ramanan, D., Dollár, P., Zitnick, C.L., 2014. Microsoft coco: Common objects

- in context, in: European conference on computer vision, Springer. pp. 740–755.
- [33] Liu, D., Zhang, H., Wu, F., Zha, Z.J., 2019a. Learning to assemble neural module tree networks for visual grounding, in: Proceedings of the IEEE/CVF International Conference on Computer Vision, pp. 4673–4682.
  - [34] Liu, X., Wang, Z., Shao, J., Wang, X., Li, H., 2019b. Improving referring expression grounding with cross-modal attention-guided erasing, in: Proceedings of the IEEE/CVF Conference on Computer Vision and Pattern Recognition, pp. 1950–1959.
  - [35] Liu, Z., Lin, Y., Cao, Y., Hu, H., Wei, Y., Zhang, Z., Lin, S., Guo, B., 2021. Swin transformer: Hierarchical vision transformer using shifted windows. International Conference on Computer Vision (ICCV) .
  - [36] Mao, J., Huang, J., Toshev, A., Camburu, O., Yuille, A.L., Murphy, K., 2016. Generation and comprehension of unambiguous object descriptions, in: Proceedings of the IEEE conference on computer vision and pattern recognition, pp. 11–20.
  - [37] Mu, Z., Tang, S., Tan, J., Yu, Q., Zhuang, Y., 2021. Disentangled motif-aware graph learning for phrase grounding, in: Proceedings of the AAAI Conference on Artificial Intelligence, pp. 13587–13594.
  - [38] Nagaraja, V.K., Morariu, V.I., Davis, L.S., 2016. Modeling context between objects for referring expression understanding, in: Computer Vision–ECCV 2016: 14th European Conference, Amsterdam, The Netherlands, October 11–14, 2016, Proceedings, Part IV 14, Springer. pp. 792–807.
  - [39] Plummer, B.A., Wang, L., Cervantes, C.M., Caicedo, J.C., Hockenmaier, J., Lazebnik, S., 2015. Flickr30k entities: Collecting region-to-phrase correspondences for richer image-to-sentence models, in: Proceedings of the IEEE international conference on computer vision, pp. 2641–2649.
  - [40] Qiu, H., Li, H., Wu, Q., Meng, F., Shi, H., Zhao, T., Ngan, K.N., 2020. Language-aware fine-grained object representation for referring expres-

- sion comprehension, in: Proceedings of the 28th ACM International Conference on Multimedia, pp. 4171–4180.
- [41] Radford, A., Kim, J.W., Hallacy, C., Ramesh, A., Goh, G., Agarwal, S., Sastry, G., Askell, A., Mishkin, P., Clark, J., et al., 2021. Learning transferable visual models from natural language supervision, in: International conference on machine learning, PMLR. pp. 8748–8763.
  - [42] Redmon, J., Farhadi, A., 2018. Yolov3: An incremental improvement. arXiv preprint arXiv:1804.02767 .
  - [43] Ren, S., He, K., Girshick, R., Sun, J., 2015. Faster r-cnn: Towards real-time object detection with region proposal networks. arXiv preprint arXiv:1506.01497 .
  - [44] Rezatofghi, H., Tsoi, N., Gwak, J., Sadeghian, A., Reid, I., Savarese, S., 2019. Generalized intersection over union: A metric and a loss for bounding box regression, in: Proceedings of the IEEE/CVF Conference on Computer Vision and Pattern Recognition, pp. 658–666.
  - [45] Stockman, G., Shapiro, L.G., 2001. Computer vision. Prentice Hall PTR.
  - [46] Touvron, H., Cord, M., Matthijs, D., Massa, F., Sablayrolles, A., Jégou, H., 2020. Training data-efficient image transformers distillation through attention. International Conference on Machine Learning, International Conference on Machine Learning .
  - [47] Vaswani, A., Shazeer, N., Parmar, N., Uszkoreit, J., Jones, L., Gomez, A.N., Kaiser, L., Polosukhin, I., 2017. Attention is all you need, in: Advances in neural information processing systems, pp. 5998–6008.
  - [48] Wang, H., Wang, Y., Zhou, Z., Ji, X., Gong, D., Zhou, J., Li, Z., Liu, W., 2018a. Cosface: Large margin cosine loss for deep face recognition, in: Proceedings of the IEEE conference on computer vision and pattern recognition, pp. 5265–5274.
  - [49] Wang, L., Li, Y., Huang, J., Lazebnik, S., 2018b. Learning two-branch neural networks for image-text matching tasks. IEEE Transactions on Pattern Analysis and Machine Intelligence 41, 394–407.

- [50] Wang, P., Wu, Q., Cao, J., Shen, C., Gao, L., Hengel, A.v.d., 2019. Neighbourhood watch: Referring expression comprehension via language-guided graph attention networks, in: Proceedings of the IEEE/CVF Conference on Computer Vision and Pattern Recognition, pp. 1960–1968.
- [51] van Wyk, G.J., Bosman, A.S., 2019. Evolutionary neural architecture search for image restoration, in: 2019 International Joint Conference on Neural Networks (IJCNN), IEEE. pp. 1–8.
- [52] Yang, F., Yang, H., Fu, J., Lu, H., Guo, B., 2020a. Learning texture transformer network for image super-resolution, in: Proceedings of the IEEE/CVF conference on computer vision and pattern recognition, pp. 5791–5800.
- [53] Yang, L., Xu, Y., Yuan, C., Liu, W., Li, B., Hu, W., 2022. Improving visual grounding with visual-linguistic verification and iterative reasoning, in: Proceedings of the IEEE/CVF Conference on Computer Vision and Pattern Recognition, pp. 9499–9508.
- [54] Yang, S., Li, G., Yu, Y., 2019a. Dynamic graph attention for referring expression comprehension, in: Proceedings of the IEEE/CVF International Conference on Computer Vision, pp. 4644–4653.
- [55] Yang, S., Li, G., Yu, Y., 2020b. Graph-structured referring expression reasoning in the wild, in: Proceedings of the IEEE/CVF Conference on Computer Vision and Pattern Recognition, pp. 9952–9961.
- [56] Yang, Z., Chen, T., Wang, L., Luo, J., 2020c. Improving one-stage visual grounding by recursive sub-query construction, in: Computer Vision—ECCV 2020: 16th European Conference, Glasgow, UK, August 23–28, 2020, Proceedings, Part XIV 16, Springer. pp. 387–404.
- [57] Yang, Z., Gong, B., Wang, L., Huang, W., Yu, D., Luo, J., 2019b. A fast and accurate one-stage approach to visual grounding, in: Proceedings of the IEEE/CVF International Conference on Computer Vision, pp. 4683–4693.
- [58] Ye, J., Lin, X., He, L., Li, D., Chen, Q., 2021. One-stage visual grounding via semantic-aware feature filter, in: Proceedings of the 29th ACM International Conference on Multimedia, pp. 1702–1711.

- [59] Ye, J., Tian, J., Yan, M., Yang, X., Wang, X., Zhang, J., He, L., Lin, X., 2022. Shifting more attention to visual backbone: Query-modulated refinement networks for end-to-end visual grounding, in: Proceedings of the IEEE/CVF Conference on Computer Vision and Pattern Recognition, pp. 15502–15512.
- [60] Young, P., Lai, A., Hodosh, M., Hockenmaier, J., 2014. From image descriptions to visual denotations: New similarity metrics for semantic inference over event descriptions. *Transactions of the Association for Computational Linguistics* 2, 67–78.
- [61] Yu, L., Lin, Z., Shen, X., Yang, J., Lu, X., Bansal, M., Berg, T.L., 2018a. Mattrnet: Modular attention network for referring expression comprehension, in: Proceedings of the IEEE Conference on Computer Vision and Pattern Recognition, pp. 1307–1315.
- [62] Yu, L., Poirson, P., Yang, S., Berg, A.C., Berg, T.L., 2016. Modeling context in referring expressions, in: *European Conference on Computer Vision*, Springer. pp. 69–85.
- [63] Yu, Z., Yu, J., Xiang, C., Zhao, Z., Tian, Q., Tao, D., 2018b. Rethinking diversified and discriminative proposal generation for visual grounding. *arXiv preprint arXiv:1805.03508* .
- [64] Zhang, C., Cao, M., Yang, D., Chen, J., Zou, Y., 2021. Cola: Weakly-supervised temporal action localization with snippet contrastive learning, in: Proceedings of the IEEE/CVF Conference on Computer Vision and Pattern Recognition, pp. 16010–16019.
- [65] Zhang, C., Yang, T., Weng, J., Cao, M., Wang, J., Zou, Y., 2022. Un-supervised pre-training for temporal action localization tasks, in: Proceedings of the IEEE/CVF Conference on Computer Vision and Pattern Recognition, pp. 14031–14041.
- [66] Zhang, H., Niu, Y., Chang, S.F., 2018. Grounding referring expressions in images by variational context, in: Proceedings of the IEEE Conference on Computer Vision and Pattern Recognition, pp. 4158–4166.
- [67] Zhu, X., Su, W., Lu, L., Li, B., Wang, X., Dai, J., 2020. Deformable detr: Deformable transformers for end-to-end object detection. *arXiv*:



## Appendix A. Ablation studies of distillation location

For better understanding, we provide a schematic diagram of the location distillation experiment here. As shown in Figure A.5, this diagram details each LOC. in the model for specific locations.

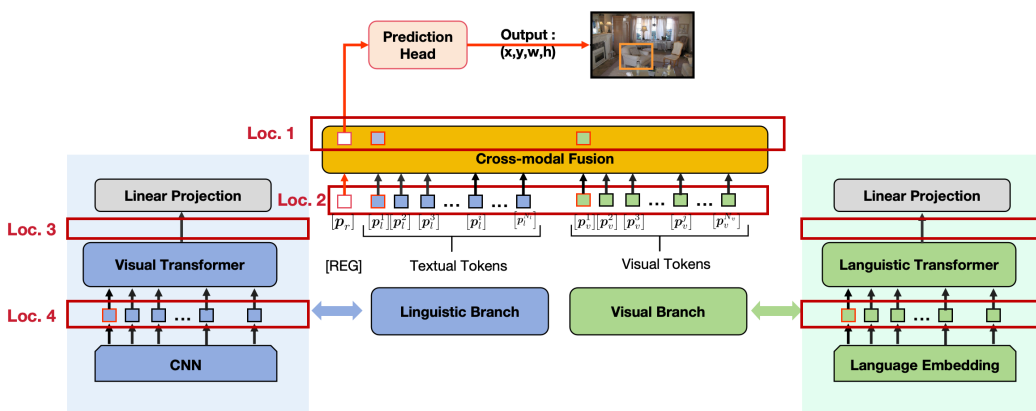


Figure A.5: A schematic diagram of the location distillation experiment

## Appendix B. Qualitative Analysis

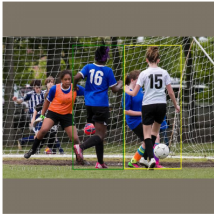
**Comparison with QRNet.** We quantitatively compare the results predicted by our model and the QRNet in Figure B.6. Green boxes are the ground truth. Yellow boxes are the predictions of our model and QRNet. We notice that our model is capable of better capturing the relevance between images and queries, thereby making accurate predictions.

**Failure Cases.** We present some typical failure cases in Figure B.7. One type of error is image blurriness. In the second example, the pants of the man in the middle are rather blurry, resembling “plaid shorts”. Another type of error is the interference from similar areas in the image. In the first example, our model struggles to distinguish between the numbers “15” and “16”. In the third example, there is a small semantic gap between “woman in black shirt and gray skirt” and “woman in black skirt and gray shirt”,



Figure B.6: Qualitative comparison with QRNet. Green boxes are the ground-truth, yellow boxes are the predictions.

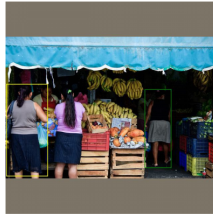
and our distillation targets only BERT's [CLS] rather than the full sequence representation for reasoning, which limits the understanding of similar areas. Similarly, in the fourth example, our model can recognize the computer but fails to grasp the "smoking" information.



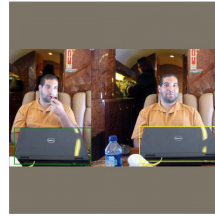
number 16



plaid shorts



woman in black  
shirt and gray skirt



computer with the  
man smoking the pipe

Figure B.7: The failure cases of our model. Green boxes are the ground-truth, yellow boxes are the predictions of our model.